


# Stopping power of dense plasmas: The collisional method and limitations of the dielectric formalism

C. F. Clauser<sup>1,2,\*</sup> and N. R. Arista<sup>1</sup>

<sup>1</sup>*Centro Atómico Bariloche and Instituto Balseiro, Comisión Nacional de Energía Atómica and Universidad Nacional de Cuyo, Av. Bustillo 9500, 8400 Bariloche, Argentina*

<sup>2</sup>*Consejo Nacional de Investigaciones Científicas y Técnicas (CONICET), Av. Bustillo 9500, 8400 Bariloche, Argentina*

 (Received 20 April 2017; revised manuscript received 26 December 2017; published 13 February 2018)

We present a study of the stopping power of plasmas using two main approaches: the collisional (scattering theory) and the dielectric formalisms. In the former case, we use a semiclassical method based on quantum scattering theory. In the latter case, we use the full description given by the extension of the Lindhard dielectric function for plasmas of all degeneracies. We compare these two theories and show that the dielectric formalism has limitations when it is used for slow heavy ions or atoms in dense plasmas. We present a study of these limitations and show the regimes where the dielectric formalism can be used, with appropriate corrections to include the usual quantum and classical limits. On the other hand, the semiclassical method shows the correct behavior for all plasma conditions and projectile velocity and charge. We consider different models for the ion charge distributions, including bare and dressed ions as well as neutral atoms.

DOI: [10.1103/PhysRevE.97.023202](https://doi.org/10.1103/PhysRevE.97.023202)

## I. INTRODUCTION

The interaction of energetic ion beams with dense and dilute plasmas is one of the fundamental processes in plasma physics and fusion research. The injection of intense atomic beams is an important method for the heating of Tokamak plasmas and provides an efficient method to reach the very high temperatures required to initiate D-T fusion reactions. In a different context, current research on inertial fusion considers the use of high-intensity ion beams as a possible alternative to produce the combination of high densities and temperatures necessary to produce the ignition of fusion reactions in small D-T pellets.

In spite of the intense activity and relevance of this field of research, quantitative comparisons between theoretical models and experiments dealing with swift ion beams are rather scarce due to the experimental difficulties in producing well-defined conditions for accurate determinations of stopping or transport coefficients through beam-plasma interactions [1,2]

From the theoretical side, two main methods have been proposed to describe the interactions between ion beams and plasmas: the dielectric formulation [3,4] and the collisional approach [5–7]. Based on the latter, further models using the transport-cross-section (TCS) approach have been described [8,9]. The purpose of the present study is to show some intrinsic limitations of the dielectric formulation when dealing with heavy ions or atoms, analyzing the physical origin of these limitations and showing how the correct solution can be obtained using the TCS approach.

The dielectric formalism to describe the energy loss of a charged particle in a medium was introduced by Fermi [3] and was further developed by various authors [4,10–12]. This formulation includes in a self-consistent way the screening

effects together with individual and collective excitations produced in the medium. The expression for the mean energy loss or *stopping power*, for a point ion with charge  $Ze$  and velocity  $v$ , is given by

$$S \equiv -\frac{dE}{dx} = \frac{2(Ze)^2}{\pi v^2} \int_0^\infty \frac{dk}{k} \int_0^{kv} d\omega \omega \operatorname{Im} \left[ \frac{-1}{\varepsilon(k, \omega)} \right], \quad (1)$$

where  $\varepsilon(k, \omega)$  is the dielectric function of the medium. Various calculations of plasma stopping powers using this approach have been given by previous authors [13–19].

A first comment that could be made here is that this expression shows a straight proportionality with the square of the ion charge. This property is akin to the results of first-order perturbation theory (such as Bethe's theory) and indicates a connection between linear response and first-order perturbation [10]. Therefore, it could be anticipated that this approximation could fail for highly charged ions.

Various properties implicit in this expression could also be considered. First, if a classical dielectric function is used [20,21], the integral in  $k$  diverges in a logarithmic way. This problem is usually circumvented by introducing a maximum value  $k_{\text{cl}}^{\text{max}} = 1/b_{\text{cl}}^{\text{min}}$ , where  $b_{\text{cl}}^{\text{min}} = Ze^2/mv^2$  is the classical Bohr collision radius associated to Rutherford scattering of electrons in close collisions with the ion ( $m$  is the electron mass). In this case the expression for the stopping power for high energies (i.e., when the ion speed is much larger than the thermal velocity of the electrons) is given by the Bohr limit [22,23]:

$$-\frac{dE}{dx} \cong \left( \frac{Ze \omega_p}{v} \right)^2 \ln \left( \frac{mv^3}{Z_1 e^2 \omega_p} \right), \quad (2)$$

where  $\omega_p = (4\pi n e^2/m)^{1/2}$  is the corresponding plasma frequency and  $n$  is the electron density of the plasma.

On the other hand, if the quantum formulation of the dielectric function is applied, for any degree of plasma degen-

\*cesar.clauser@ib.edu.ar

eracy [24], an upper cutoff in the  $k$  integral is automatically applied, which arises from the limitation in the maximum momentum transfer that can occur in the excitation of a single electron by the moving particle. For high-energy particles the maximum momentum transfer is given by  $\hbar k_{\text{qm}}^{\text{max}} \cong 2mv$  (see Appendix A). In this case the high-energy behavior of the stopping power is given by the Bethe limit [12]:

$$-\frac{dE}{dx} \cong \left( \frac{Ze\omega_p}{v} \right)^2 \ln \left( \frac{2mv^2}{\hbar\omega_p} \right). \quad (3)$$

Over the years, there have been many attempts to solve the apparent discrepancy between these two results. Most notably, Bloch obtained a closed solution that bridges the gap between the classical and the quantum (perturbative) limits in a very elegant way, but only in the limit of high energies [25].

So far the usual way to implement a similar solution in the classical dielectric formulation is by introducing in an *ad hoc* way some appropriate upper cutoff in the  $k$  integral, considering the classical value of  $k_{\text{cl}}^{\text{max}}$  when  $Ze^2/\hbar v > 1$ , and the quantum value  $k_{\text{qm}}^{\text{max}}$  in the opposite case (i.e., using always the lower value between  $k_{\text{cl}}^{\text{max}}$  and  $k_{\text{qm}}^{\text{max}}$ ) [16,17]. On the other hand, if the quantum dielectric function is used, the only correction to be explicitly considered is the classical one (when appropriate), since, as said before, the quantum cutoff of the  $k$  integral is implicitly included in the properties of the dielectric function.

These considerations can be extended to smaller ion velocities in a heuristic way by replacing

$$v \longrightarrow \bar{v}_r = \sqrt{v^2 + v_s^2}, \quad (4)$$

where  $v_s$  is a mean kinetic speed of the plasma electrons. This proposal has been already made for classical plasmas [16,17], taking  $v_s = v_{\text{th}}$ , and it was also extended to degenerate plasmas [26] approximating  $v_s = \sqrt{v_{\text{th}}^2 + v_F^2}$ . Here  $v_{\text{th}}$  and  $v_F$  are the thermal and Fermi velocity, respectively (see below).

However, as we will show in this work, the simple use of this procedure to extend the  $k$  cutoff breaks down in some cases, in particular, in the case of slow heavy projectiles. It could also be shown that in all cases, the method that is free of inconsistencies, and in addition provides a well-behaved solution that incorporates nonlinear effects, is the transport cross section approach based on quantum scattering theory [9].

The paper is organized as follows: in Sec. II we present the plasma description. In Secs. III and IV we describe the collisional approach and the dielectric formulation, respectively, and in Sec. V we review the interaction potentials to be considered. In Sec. VI we present the results and show the limitations of the dielectric formalism. Finally, we summarize the present work in the conclusions. There are also two appendices to support some important results used in the present work.

## II. PLASMA DESCRIPTION

The velocity distribution of a free electron plasma is given, in the general case, by the Fermi-Dirac (FD) statistics, which

gives the following distribution function:

$$f_{\text{FD}}(v_e) = \frac{2m^3}{(2\pi\hbar)^3 n} \frac{1}{1 + e^{\beta(E-\mu)}}. \quad (5)$$

Here  $\beta = 1/T$  (temperature  $T$  is given in energy unit),  $n$  is the density,  $m$  is the electron mass, and  $E = mv_e^2/2$  is the electron energy. The chemical potential  $\mu$  can be calculated according to Ref. [24]. The distribution function is normalized as

$$\int f_{\text{FD}}(v_e) d^3v_e = 1. \quad (6)$$

The degree of degeneracy can be characterized by the parameter  $\theta = T/E_F$ , with  $E_F = \hbar^2(3\pi^2 n)^{2/3}/2m$  being the Fermi energy.

For a description of the screening properties of the electron gas it is useful to define an average electron velocity  $v_s$  using the FD distribution by the following relation [24]:

$$\frac{1}{v_s^2} = 4\pi \int_0^\infty f_{\text{FD}}(v_e) dv_e. \quad (7)$$

This reproduces the Thomas-Fermi limit  $v_s \rightarrow v_F/\sqrt{3}$  for quantum plasmas ( $\theta \ll 1$ ) and the Debye limit  $v_s \rightarrow v_{\text{th}} = \sqrt{T/m}$  for classical plasmas ( $\theta \gg 1$ ). Hence, this definition gives an adequate electron velocity without approximating it as we mentioned in the Introduction.

In the classical limit of nondegenerate plasmas ( $\theta \gg 1$ ) the distribution function takes the form of the Maxwell-Boltzmann (MB) distribution:

$$f_{\text{MB}}(v_e) = \frac{1}{(2\pi v_{\text{th}}^2)^{3/2}} \exp\left(-\frac{v_e^2}{2v_{\text{th}}^2}\right). \quad (8)$$

We can also note that for a wide range of interest, including dense regions, the MB distribution can be conveniently modified and used instead of the FD distribution. The usual MB statistic uses the limit  $v_s \rightarrow v_{\text{th}}$ , but here we propose to keep  $v_s$  [calculated from Eq. (7)] instead of  $v_{\text{th}}$  and labeling the corresponding distribution with MB\*, which yields the distribution

$$f_{\text{MB}^*}(v_e) = \frac{1}{(2\pi v_s^2)^{3/2}} \exp\left(-\frac{v_e^2}{2v_s^2}\right). \quad (9)$$

Figure 1 compares this approximation with the exact FD distribution for a partially degenerated plasma with  $\theta = 1.2$  ( $n = 10^{23} \text{ cm}^{-3}$  and  $T = 10 \text{ eV}$ ), conditions that will be used below as a reference case.

## III. SEMICLASSICAL PARTIAL WAVE SCATTERING (SPWS) METHOD

This method was presented in a general form in Ref. [27] and was applied in a previous work [9] to calculate the energy loss of ions in plasmas, showing the oscillation of the stopping power as a function of the projectile atomic number.

The main quantity in this description is the transport cross section (TCS), which, according to the quantum scattering theory, may be written in terms of the scattering phase shifts  $\delta_l$  as

$$\sigma_{\text{tr}} = \frac{4\pi}{q^2} \sum_l (l+1) \sin^2(\delta_l - \delta_{l+1}). \quad (10)$$

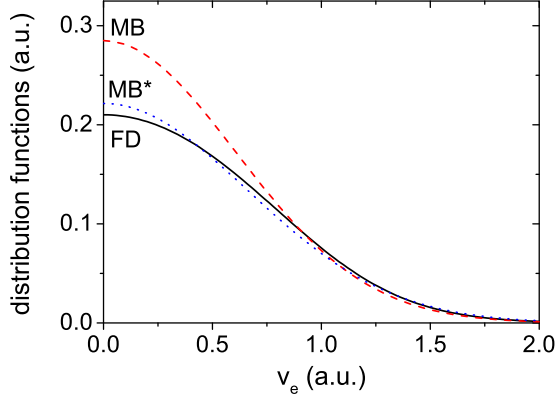


FIG. 1. Distribution functions for a  $n = 10^{23} \text{ cm}^{-3}$  and  $T = 10 \text{ eV}$  plasma. FD denotes the Fermi-Dirac, MB the Maxwell-Boltzmann, and MB\* the modified Maxwell-Boltzmann.

Here  $q$  refers to the wave number corresponding to the scattered electron with relative velocity  $v_r = |\mathbf{v}_e - \mathbf{v}| = \hbar q/m$ . The exact way to find the phase shifts is by solving the Schrödinger equation, while the semiclassical WKB approximation gives an explicit expression for the phase shifts. In this scheme, and for a given spherically symmetric potential  $V(r)$ , the phase shifts are calculated by the following integral [28]:

$$\delta_l = \int dr \sqrt{q^2 - \frac{(l+1/2)^2}{r^2} - \frac{2m}{\hbar^2} V(r)} - \int dr \sqrt{q^2 - \frac{(l+1/2)^2}{r^2}}. \quad (11)$$

This approximation was employed before by Maynard *et al.* [29], but they made only a limited use of it for large quantum numbers  $l$ . However, it has been tested as an excellent approximation to the full quantum-mechanical solution [27] and was compared with experimental results in solid targets showing a very good agreement [9]. In (11) the integrals go over the range where the corresponding integrand functions are positive.

To obtain the stopping power in the scattering theory we must integrate over all relative velocities  $v_r$  (between the electrons and the moving ion) and then, over the plasma distribution function, as [8]

$$S(v) = \frac{\pi m n}{v^2} \int_0^\infty dv_e v_e f_{\text{FD}}(v_e) G(v, v_e) \quad (12)$$

with

$$G(v, v_e) = \int_{|v-v_e|}^{v+v_e} dv_r v_r^4 \sigma_{\text{tr}}(v_r) \left(1 + \frac{v^2 - v_e^2}{v_r^2}\right). \quad (13)$$

Moreover, using the MB\* approximation described in Sec. II it is possible to perform one of the integrals involved in the stopping power (see Appendix B) and obtain

$$S = \frac{2\pi m n}{(2\pi v_s^2)^{3/2}} \int_0^\infty dv_r v_r^4 \sigma_{\text{tr}}(v_r) \times \exp\left(\frac{v^2 + v_r^2}{2v_s^2}\right) I\left(\frac{v v_r}{v_s}\right), \quad (14)$$

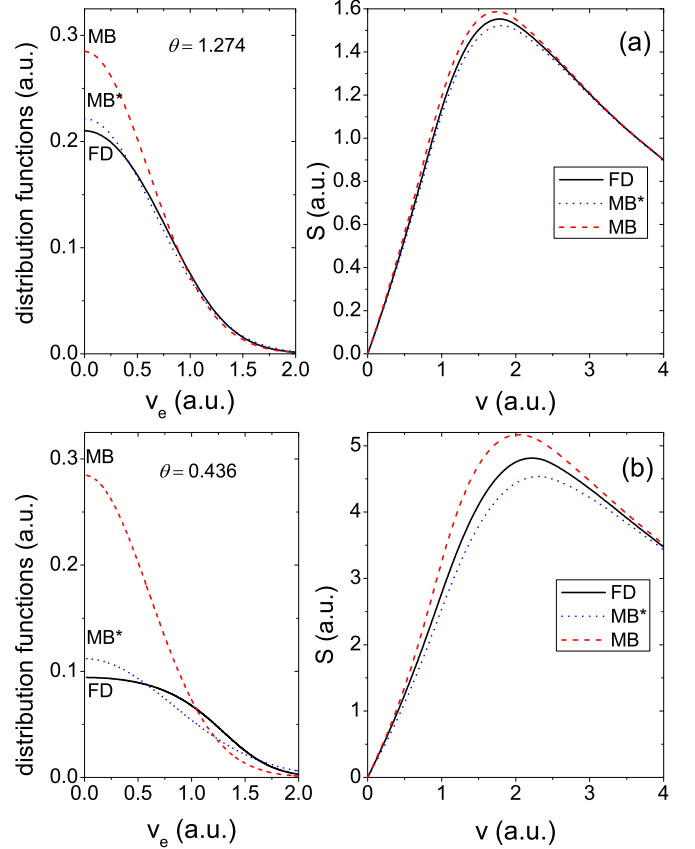


FIG. 2. Distribution functions and their corresponding SPWS stopping, for two plasma conditions: (a)  $n = 10^{23} \text{ cm}^{-3}$  ( $\theta = 1.274$ ) and (b)  $n = 5 \times 10^{23} \text{ cm}^{-3}$  ( $\theta = 0.436$ ). In both cases the temperature is  $T = 10 \text{ eV}$  and the projectile is a stripped ion with  $Z = 5$ . FD, MB, and MB\* refer to Fermi-Dirac, Maxwell-Boltzmann, and the modified Maxwell-Boltzmann, respectively.

where

$$I(\beta) = \frac{1}{\beta^2} [(1 + \beta)e^{-\beta} - (1 - \beta)e^{\beta}] \quad (15)$$

and  $\beta = v v_r / v_s^2$ . This expression presents a great computational advantage, as discussed in Appendix B.

Figure 2 shows the distribution functions FD, MB, and MB\* (left side) and the SPWS stopping for each distribution (right side) for two plasma conditions: (1)  $n = 10^{23} \text{ cm}^{-3}$  ( $\theta = 1.274$ ) and (2)  $n = 5 \times 10^{23} \text{ cm}^{-3}$  ( $\theta = 0.436$ ). In both cases the temperature is  $T = 10 \text{ eV}$  and the projectile is a stripped ion with  $Z = 5$  (see Sec. V A for the potential description). We can note that the MB\* approximation produces a significant improvement when comparing it with the MB approximation and the FD results.

#### IV. DIELECTRIC FORMALISM (DF) METHOD

The dielectric function of an electron gas, described by Eq. (5), can be parametrized for all degrees of plasma degeneracy by the expression [24]

$$\varepsilon(k, \omega) = 1 + \frac{1}{4\pi k_F a_0 z^3} [g(u+z) - g(u-z)] \quad (16)$$

in terms of the wave number  $k$  and frequency  $\omega$ . Here  $a_0$  is the Bohr radius,  $k_F = mv_F/\hbar = (3\pi^2n)^{1/3}$  is the Fermi wave number,  $u = \omega/kv_F$ ,  $z = k/2k_F$  and

$$g(x) = \int_0^\infty \frac{y dy}{e^{Dy^2 - \beta\mu} + 1} \ln \left( \frac{x+y}{x-y} \right), \quad (17)$$

where  $D = 1/\theta = E_F/T$  is the degeneracy parameter.

For calculation purposes it is also convenient to separate the real and imaginary parts of the dielectric function,  $\varepsilon = \varepsilon_1 + i\varepsilon_2$  [24], as

$$\varepsilon_1(k, \omega) = 1 + \frac{1}{4\pi k_F a_0 z^3} [\tilde{g}(u+z) - \tilde{g}(u-z)], \quad (18)$$

where

$$\tilde{g}(x) = \int_0^\infty \frac{y dy}{e^{Dy^2 - \beta\mu} + 1} \ln \left| \frac{x+y}{x-y} \right| \quad (19)$$

and

$$\varepsilon_2(k, \omega) = \frac{1}{8k_F a_0 z^3} \theta \ln \left( \frac{1 + e^{\beta\mu - D(u-z)^2}}{1 + e^{\beta\mu - D(u+z)^2}} \right). \quad (20)$$

The expression for the stopping power in the dielectric formulation already anticipated in Eq. (1) applies only to the case of a point ion of charge  $Ze$ . That expression can be generalized for the more general case of an ion with charge  $Q$ , carrying  $N_e = Z - Q/e$  bound electrons, in the form [30]

$$S(v) = \frac{2}{\pi v^2} \int_0^{k_{\max}} \frac{dk}{k} [Ze + \rho_e(k)]^2 \int_0^{kv} d\omega \omega \operatorname{Im} \left[ \frac{-1}{\varepsilon(k, \omega)} \right], \quad (21)$$

where  $\rho_e(k)$  is the Fourier transform of the electron charge density  $\rho_e(r)$  corresponding to the  $N_e$  bound electrons. Obviously, for neutral projectiles we have  $Q = 0$ . Even though the  $k$ -integral converges for  $k \rightarrow \infty$  (and it is usually presented in this way), a cutoff  $k_{\max}$  was added to emphasize the discussion in Sec. VI.

Explicit expressions for these quantities, using particular models for the ion charge distributions, will be given below.

## V. PROJECTILE MODELS AND INTERACTION POTENTIALS

In this section we explore some typical atomic models to test the previous stopping formulations. On one hand, the SPWS method [Eq. (12)] uses the interaction potential  $V(r)$  as the basic ingredient of the calculation. On the other hand, the DF method [Eq. (21)] uses the Fourier transform of the electron charge density  $\rho_e(k)$  in vacuum because plasma screening effects are introduced implicitly through the dielectric function. Hence, we give here a brief review of both descriptions for the considered projectile models.

### A. Yukawa potential and plasma screening

The first case we consider is the interaction of a point charge  $Q$  with a plasma electron. The most simple model of a screened potential is the well-known Yukawa one [20],

$$V_Y(r) = -\frac{Qe}{r} e^{-r/\lambda}, \quad (22)$$

where  $\lambda$  is the plasma screening length. This potential was originally obtained in the static projectile velocity limit ( $v \ll v_s$ ) and for a classical plasma. However, this potential can be extended to all plasma degeneracies, and, in this static limit, the plasma screening length is given by [24]

$$\lambda_s = \frac{v_s}{\omega_p}, \quad (23)$$

where  $v_s$  is defined by Eq. (7). On the other hand, for high-projectile velocities, the dynamical screening length is [31]

$$\lambda_{ad}(v) = \frac{v}{\omega_p}. \quad (24)$$

Hence, for a wide range of velocities we can use the following standard interpolation [9,26]:

$$\lambda(v) \approx \frac{\bar{v}_r}{\omega_p} = \frac{\sqrt{v_s^2 + v^2}}{\omega_p}. \quad (25)$$

The Yukawa potential [Eq. (22)] is used for the calculation of the energy loss using the SPWS method. For the dielectric formalism, we need the Fourier transform of the electron charge density,  $\rho_e(k)$ , according to Eq. (21). But this point charge  $Q$  corresponds to a null external electron charge density, since the induced charge is implicitly contained in the dielectric response. Hence, for the DF calculation, we simply have  $\rho_e(k) = 0$ .

### B. Molière potential

Let us consider the more general case of a projectile of nuclear charge  $Ze$  and  $N_e$  bound electrons ( $Q/e = Z - N_e$ ). We define the ionization degree as

$$\eta = \frac{Q}{Ze}. \quad (26)$$

An important statistical model for neutral atoms is the potential proposed by Molière [32], which is a fit of the Thomas-Fermi model [28]. This potential was developed for neutral atoms, but it is possible to modify it in order to include partially ionized atoms. This modification was proposed in Ref. [33] and takes the form

$$V_M(r) = -\frac{Ze^2\eta}{r} e^{-r/\lambda} - \frac{Ze^2}{r} \sum_{i=1}^3 A_i e^{-r/a_i}. \quad (27)$$

The values of  $a_i$  are those of the usual Molière potential, while the values of  $A_i$  are approximately adjusted to represent an ion with  $N_e$  bound electrons, as described in Ref. [33]. They satisfy the normalization condition  $A_1 + A_2 + A_3 = N_e/Z$ . In the limit  $\lambda \rightarrow \infty$ , Eq. (27) yields the potential of the ion in vacuum. We also note that similar potentials have been proposed in the literature (see, for example, Ref. [34]).

The corresponding Fourier transform of the charge density of the  $N_e$  bound electrons is

$$\rho_e(k) = -Ze \sum_{i=1}^3 \frac{A_i \alpha_i^2}{k^2 + \alpha_i^2}, \quad (28)$$

where  $\alpha_i = 1/a_i$ . As in the previous case, the potential, given in this case by Eq. (27), is used for the SPWS method, while the expression given by Eq. (28) is used in the DF calculation.

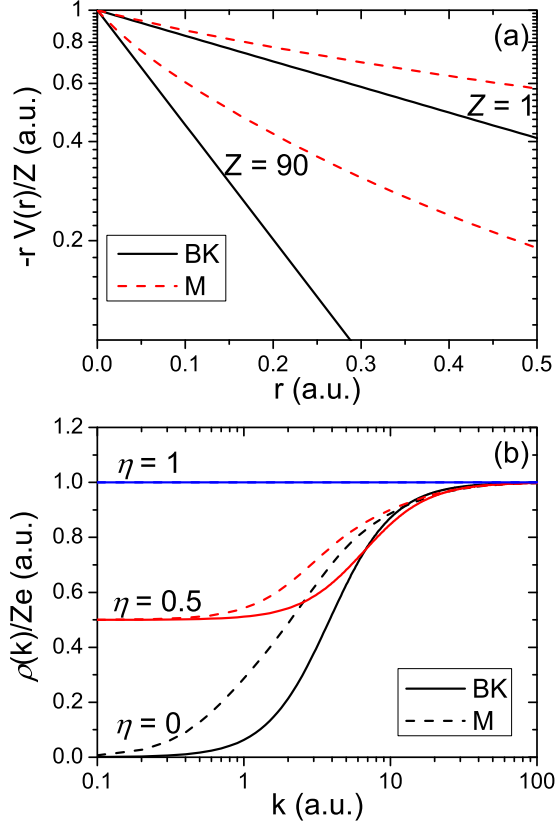


FIG. 3. Comparison of the Brandt-Kitagawa (BK) and Molière (M) projectile models. In (a) we show the potentials, for neutral atoms ( $\eta = 0$ ), as a function of the radial coordinate, and in (b) we show the charge density in momentum space, for different ionization degrees.

### C. Brandt-Kitagawa model

Another atomic model was proposed by Brandt and Kitagawa (BK) [30]. The BK is a model for the electron cloud in the projectile of the form

$$\rho_{e,BK}(r) = -\frac{N_e e}{4\pi\Lambda^3} \frac{\Lambda}{r} e^{-r/\Lambda}, \quad (29)$$

where  $N_e$  is the number of bound electrons and  $\Lambda$  is given by

$$\Lambda(Z, N_e) = \frac{0.48 N_e^{2/3}}{Z - \frac{1}{7} N_e} a_0. \quad (30)$$

The Fourier transform of the electron charge density, used for the DF calculation, is in this case

$$\rho_{e,BK}(k) = -\frac{N_e e}{1 + (k\Lambda)^2}, \quad (31)$$

and the ion potential, used in the SPWS calculation, is given by

$$V_{BK}(r) = -\frac{Ze^2\eta}{r} e^{-r/\lambda} - \frac{N_e e^2}{r} e^{-r/\Lambda}. \quad (32)$$

Figure 3 compares in (a) the BK and the Molière potentials while in (b), the Fourier transform of the total projectile charge density,  $\rho(k) = Ze + \rho_e(k)$ . We can see that the BK potential is much more localized than the Molière one. In particular, large differences are observed for neutral atoms with  $Z \gg 1$ .

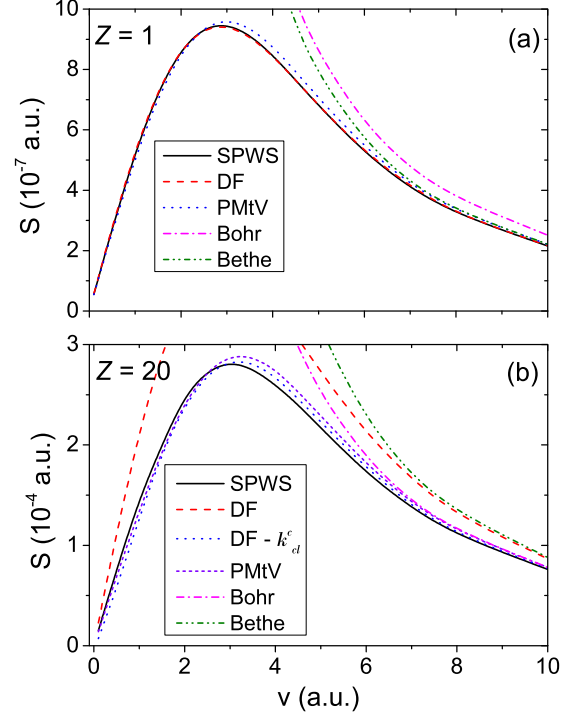


FIG. 4. Comparison of the stopping power for different calculation methods. The plasma conditions are  $n = 10^{18} \text{ cm}^{-3}$  and  $T = 100 \text{ eV}$  (classical plasma). In (a) we can observe the concordance between the SPWS, DF, and PMtV calculations. In (b) we show that the plain DF calculation yields a very large overestimation, but when the Coulomb classical cutoff is applied (DF- $k_{cl}^c$ ) it becomes in good agreement with the SPWS and PMtV calculations.

Finally we notice that, in addition to the basic potentials considered here, more advanced potentials have been studied [35,36], taking into account shell and subshell effects. Moreover, the consideration of neutral or partially ionized projectiles in dense plasma targets could add an inelastic stopping contribution [37]. However, these corrections do not affect the main goal of the present work.

## VI. RESULTS

### A. Stripped ions

Let us consider, as a first case, the stopping of stripped ions in a classical plasma ( $T = 100 \text{ eV}$  and  $n = 10^{18} \text{ cm}^{-3}$ ), as a function of the projectile velocity. Figure 4 shows the two main approaches described above: the SPWS and DF methods. In this example, we consider stripped ions in order to include the Bohr and Bethe limits as well as an analytical calculation performed by Peter and Meyer-ter-Vehn (PMtV) [16] which uses a dielectric formalism with a classical dielectric function.

For the DF method, and as we mentioned in the Introduction, a  $k$  cutoff must be imposed to avoid divergences (for both Bethe and Bohr limits). Using Eq. (4) it is possible to extend the usual Bohr cutoff,  $k_{cl}^{\max}$  (mentioned in the Introduction and which was obtained in the high-velocity regime) to the whole velocity range as proposed in Ref. [16],

$$k_{cl}^c = \frac{m\bar{v}_r^2}{Ze^2}, \quad (33)$$

where the superscript refers to the Coulomb potential [see Eqs. (36) and (37)] and the subscript refers to the fact that it is a classical cutoff. We will refer to this limit as the Coulomb classical cutoff. We also use the same criterion for the Bethe cutoff,  $k_{\text{qm}}^{\text{max}}$ , to obtain

$$k_{\text{qm}} = \frac{2m\bar{v}_r}{\hbar}, \quad (34)$$

which we now refer to as quantum mechanical ( $qm$ ) cutoff. Then the usual parameter that separates both limits is [8,16]

$$\gamma \equiv \frac{1}{2} \frac{k_{\text{qm}}}{k_{\text{cl}}^c} = \frac{Ze^2}{\hbar\bar{v}_r}. \quad (35)$$

Thus, for highly charged ions, the classical cutoff is appropriate, while, for low-charged ions, the quantum limit is the correct one.

Hence, the calculations with the DF comprise two alternatives: (1) We have the classical dielectric formulation, where the classical dielectric function is used in Eq. (21). This approach has been described in detail in Ref. [16]; in this case the value of  $k_{\text{max}}$  has to be specified as an external parameter, so that if  $\gamma > 1$  the classical value of Eq. (33) is used, while if  $\gamma < 1$  the quantum value of Eq. (34), applies. (2) We also have the quantum dielectric formulation (QDF), described in Sec. IV. In this case the quantum cutoff behavior is already contained as an implicit property of the quantum dielectric function [Eqs. (18)–(20)]. Therefore in this case we only need to incorporate the transition to the classical regime, which is done by using in Eq. (21) the  $k_{\text{max}}$  value given by Eq. (33). This provides in all cases a smooth transition between the classical and the quantum regimes. Notice that these criteria apply only for bare ions with charge  $Ze$ . The case of neutral or partially dressed ions is not covered by these prescriptions; these cases are discussed in Sec. VIB.

By contrast, the SPWS method applies to atoms or ions with any charge state. It may also be noticed that alternative methods based on unified or convergent kinetic theories [38,39] have more particular restrictions that apply when the perturbation covers a wide range of impact parameters or momentum transfers. In particular, the constraining criterion being: close impact radius  $\ll$  screening radius. This criterion fails in many cases, such as for dense plasma and slow heavy ions, as will be discussed below.

Figure 4(a) shows the results for the case  $Z = 1$  where the Bethe limit, given by Eq. (3), is appropriate. In this figure, the DF and the PMtV calculations are in excellent agreement with the SPWS method and it is not necessary to include a cutoff in the  $k$ -integral since it is implicitly included in the dielectric function [Eq. (20)] (see Appendix A for further details). We also include the Bohr limit, given by Eq. (2), to illustrate its overestimated values.

On the other hand, Fig. 4(b) shows the  $Z = 20$  case in which the classical cutoff criterion is appropriate ( $\gamma > 1$ ) for the whole velocity range considered. In this figure, we include two curves corresponding to the DF method: with and without the  $k_{\text{cl}}^c$  cutoff. We can observe that without this cutoff, the DF method yields a stopping which is highly overestimated and matches the Bethe limit, as expected. On the other hand, when applying the Coulomb classical cutoff in the  $k$  integral of Eq. (1), the DF method yields an excellent agreement with the

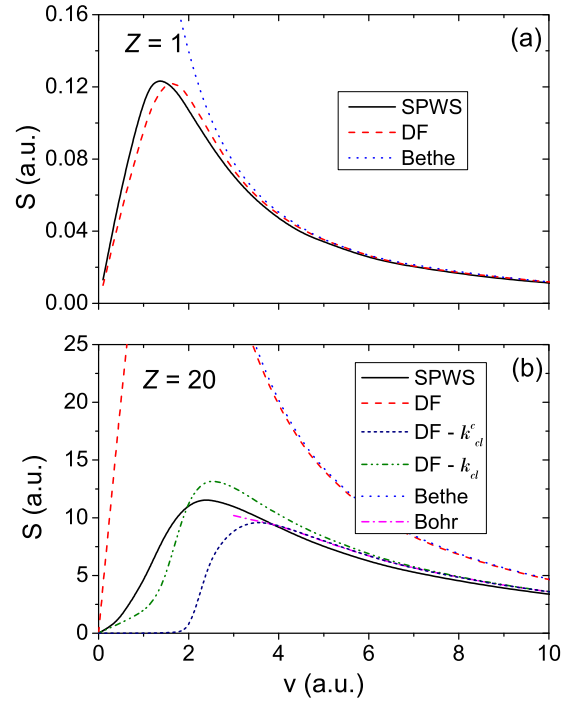


FIG. 5. Comparison of the stopping power for different calculation methods. The plasma conditions are  $n = 10^{23} \text{ cm}^{-3}$  and  $T = 10 \text{ eV}$  (partially degenerate plasma). In (a) both models (SPWS and DF) are in agreement, but in (b) we can observe that the Coulomb  $k_{\text{cl}}^c$  cutoff approach fails at low velocities.

SPWS method and the PMtV stopping. Hence, we note here the importance of the classical cutoff, when it is appropriate, in the DF method, to give an adequate behavior. It is important to note here that, as we showed in a previous work [9], the SPWS method incorporates both limits implicitly.

As a second case, we consider the stopping power of stripped ions in a partially degenerate plasma ( $\theta = 1.2$ ,  $n = 10^{23} \text{ cm}^{-3}$ , and  $T = 10 \text{ eV}$ ), which is shown in Fig. 5. As in the previous case, in Fig. 5(a) we show results for  $Z = 1$  (Bethe limit), while in (b) we show the case  $Z = 20$  (Bohr limit). We can observe in Fig. 5(a) that there is a good agreement between the DF and SPWS methods and both tend to the Bethe limit as expected. On the other hand, a very different behavior is observed in Fig. 5(b) for a point charge with  $Z = 20$ . Here the unrestricted DF method highly overestimates the stopping values, as in Fig. 4(b), matching the inappropriate Bethe limit at high energies. However, when the Coulomb classical cutoff  $k_{\text{cl}}^c$  is used, the DF result (indicated by DF- $k_{\text{cl}}^c$  in the figure) shows a very good behavior at high energies, matching the expected Bohr behavior, but it drops in a very anomalous way at low energies. In particular, the stopping calculated with this method (DF- $k_{\text{cl}}^c$ ) vanishes at low projectile velocities ( $v \lesssim 2 \text{ a.u.}$ ). The curve labeled DF- $k_{\text{cl}}^c$  will be discussed later. A similar effect was noted previously by Zwicknagel *et al.* [26] and Maynard *et al.* [29]. The explanation of this anomalous behavior will be considered in detail next.

The  $k_{\text{cl}}^c$  limit's failure in partially and degenerate plasmas stems from the fact that it was derived from the closest impact parameter behavior using a pure Coulomb potential (Rutherford scattering). In particular, it can be obtained from

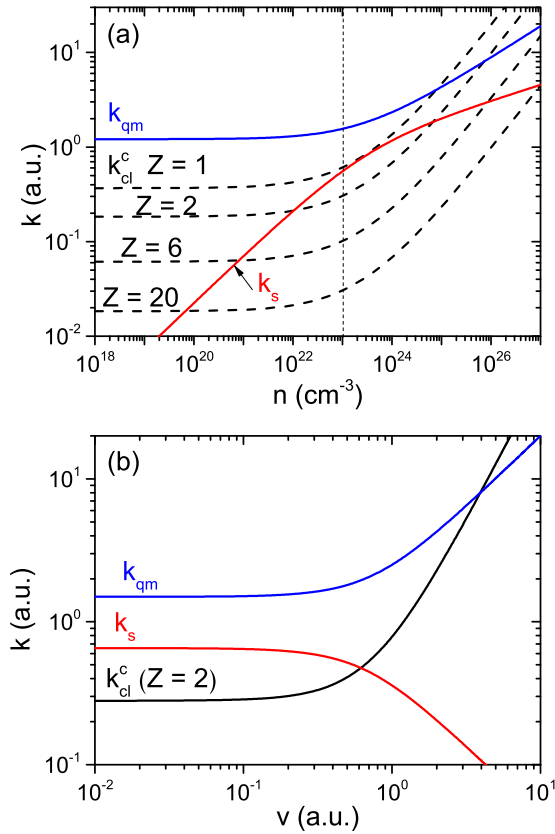


FIG. 6. Comparison between  $k_{\text{qm}}$ ,  $k_{\text{cl}}^c$ , and  $k_s$ . In (a) we show them as a function of plasma density, for  $T = 10 \text{ eV}$  and  $v = 0$ . In (b) we show the same  $k$  limit values for a fixed plasma density  $n = 10^{23} \text{ cm}^{-3}$  (and  $T = 10 \text{ eV}$ ) but varying the projectile velocity  $v$ . In both cases the  $k_s > k_{\text{cl}}^c$  condition is not physically correct.

the matching between kinetic and potential energies

$$\frac{1}{2} m \bar{v}_r^2 = \frac{Z e^2}{r_0}, \quad (36)$$

and then, defining

$$b_{\text{cl}}^c = \frac{1}{2} r_0, \quad (37)$$

we retrieve the previous definition  $k_{\text{cl}}^c = 1/b_{\text{cl}}^c$ , given by Eq. (33). But for these plasma temperature and density conditions, the screening modifies substantially the potential behavior, and this classical limit for bare ions no longer represents a typical close impact parameter. Moreover, in such cases and because the potential is strongly screened,  $b_{\text{cl}}^c$  becomes larger than the screening length,  $\lambda(v)$ , which is normally considered as an approximate upper impact parameter limit. Hence, this situation is physically inconsistent because the electrons can penetrate more than the classical impact parameter before they are deflected by the ion potential.

To illustrate this situation, Fig. 6(a) shows  $k_{\text{qm}}$ ,  $k_{\text{cl}}^c$  and the screening parameter  $k_s = 1/\lambda(v)$  as a function of plasma density in the low-velocity limit ( $v \ll v_s$ ) and for  $T = 10 \text{ eV}$ . We can observe that the previous studied case [Fig. 5(b)] corresponds to  $k_s > k_{\text{cl}}^c$  [i.e.,  $b_{\text{cl}}^c > \lambda(v)$ ], a situation that is not physically correct, and hence there is no contribution to the integral calculation when the Coulomb classical cutoff is used.

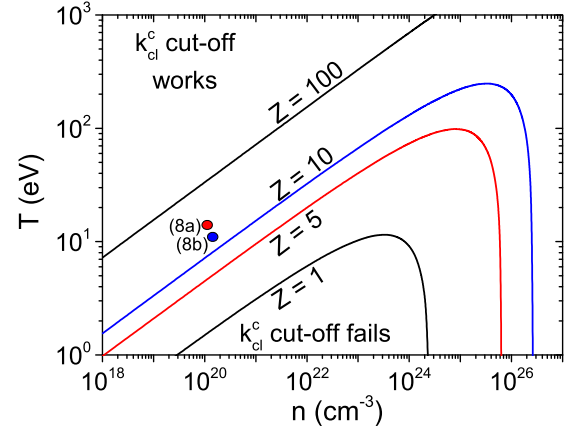


FIG. 7.  $k_s \sim k_{\text{cl}}^c$  condition in the static limit ( $v \ll v_s$ ) and for different charges  $Z$  (bare ions). The curves separate the regions in which the Coulomb  $k_{\text{cl}}^c$  cutoff can be used.

This is the reason for the sudden drop of the DF- $k_{\text{cl}}^c$  stopping curve when  $v \sim 2 \text{ a.u.}$  in Fig. 5(b). In addition, Fig. 6(b) shows the same  $k$  limits, but now, as a function of the projectile velocity and for the same plasma conditions used in Fig. 5. In this case, we use  $Z = 2$  for the classical cutoff in order to show a case where the quantum cutoff is appropriate. It is clear from Fig. 6(b) that for  $v > 4 \text{ a.u.}$  (high speed) the  $k_{\text{qm}}$  prevails (i.e.,  $k_{\text{qm}} < k_{\text{cl}}^c$ ) while for  $v < 4 \text{ a.u.}$   $k_{\text{cl}}^c$  applies. However, for  $v < 0.6$  this Coulomb classical cutoff becomes unrealistic ( $k_{\text{cl}}^c < k_s$ ), and there is no simple way to amend the dielectric formulation.

Taking into account Eqs. (36) and (37), a new classical cutoff criterion is here proposed. We apply again the energy-matching condition to determine a typical collision distance  $r_0$  in terms of the actual scattering potential:

$$\frac{1}{2} m \bar{v}_r^2 = V(r_0), \quad (38)$$

and, in correspondence with Eq. (37), we define the new classical cutoff

$$k_{\text{cl}} = \frac{2}{r_0}. \quad (39)$$

In the case of stripped ions, we can use the Yukawa potential to obtain a more plausible value of  $r_0$ :

$$\frac{1}{2} m \bar{v}_r^2 = \frac{Z e^2}{r_0} e^{-r_0/\lambda}. \quad (40)$$

The stopping power, calculated by Eq. (1), using this cutoff is shown in Fig. 5(b) with the label DF- $k_{\text{cl}}$ . Although the result still differs from the SPWS calculation (considered the best result) we notice a significant improvement with respect to the straight classical (Coulomb) criterion. This example shows that the reason for the failure of the dielectric calculation arises from the inappropriate cutoff criterion.

To investigate the region in which the Coulomb classical cutoff works well (in the whole velocity range), we assume  $\lambda \gg r_0$ , and then the first-order expansion of Eq. (40) in powers of  $r_0/\lambda$  yields

$$k_{\text{cl}} = k_{\text{cl}}^c + \frac{2}{\lambda}. \quad (41)$$

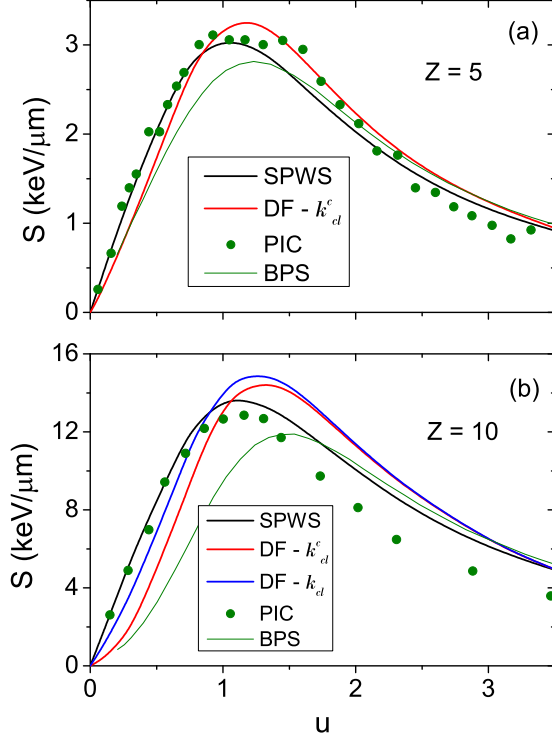


FIG. 8. Comparison of the SPWS and DF stopping with other formalism: a particle-in-cell code (PIC) and the BPS stopping (see the text). Here  $u = v/\sqrt{3T/m}$  is a normalized velocity. The plasma conditions are (a)  $n = 1.1 \times 10^{20} \text{ cm}^{-3}$ ,  $T = 14 \text{ eV}$  and (b)  $n = 1.4 \times 10^{20} \text{ cm}^{-3}$ ,  $T = 11 \text{ eV}$ .

Hence, for stripped ions we can define the condition

$$k_{cl}^c \sim k_s = \lambda^{-1}(v) \quad (42)$$

as a limiting criterion that separates the regions in which the Coulomb classical cutoff is appropriate. Figure 7 shows this condition in the static limit ( $v \ll v_s$ ), for various projectile charges  $Z$ , as a function of the plasma temperature and density. Basically, the Coulomb classical cutoff prescription works well for dilute or moderate density plasmas at high temperatures, and the restrictions increase with the charge  $Z$ .

Finally, we compare, in Fig. 8 the SPWS and DF method with more recent stopping calculations: the BPS model [40] and a particle-in-cell (PIC) code [26] (data extracted from [41]). The figure shows the stopping as function of the nor-

malized velocity  $u = v/\sqrt{3T/m}$  for the following conditions: (a)  $n = 1.1 \times 10^{20} \text{ cm}^{-3}$ ,  $T = 14 \text{ eV}$ ,  $Z = 5$  and (b)  $n = 1.4 \times 10^{20} \text{ cm}^{-3}$ ,  $T = 11 \text{ eV}$ ,  $Z = 10$ . As may be observed, the SPWS calculations yield the best agreement with the PIC simulations at low and intermediate velocities. All the calculations in Fig. 8(a), as well as the PIC results, converge to the correct Bethe-Bloch limit at high velocities, whereas in Fig. 8(b) the PIC results do not reach that limit; this failure can be attributed to an insufficient size of the simulation cell, as compared with the interaction range, according to the explanation given in Ref. [26]. Figure 8 also shows the DF method. From the conditions in Fig. 8(a) we have that the use of the  $k_{cl}^c$  cutoff gives an adequate behavior, and its replacement by  $k_{cl}$  (not shown in the figure) does not produce an improvement. However, in Fig 8(b), the use of the  $k_{cl}$  cutoff clearly improves the DF result. This can be understood taking into account Fig. 7. In the latter, the plasma conditions of Figs. 8(a) and 8(b) are indicated by the small circles labeled as “(8a)” and “(8b),” respectively. As can be observed, the condition (8a) is far enough from the curve  $Z = 5$ , and hence, the Coulomb classical cutoff is appropriate. On the other hand, the condition (8b) is close enough from the curve  $Z = 10$ , and hence, the Coulomb classical cutoff fails.

## B. Neutral projectiles

The fact that the Coulomb classical cutoff criterion fails and hence the DF method becomes unreliable, for high-density plasmas and for slow highly charged ions, also has important consequences for neutral and partially ionized projectiles. Figure 9 shows the energy loss of a carbon projectile, for different ionization degrees, in a plasma of  $n = 10^{23} \text{ cm}^{-3}$  and  $T = 10 \text{ eV}$ . In Figs. 9(a) and 9(b) we compare the SPWS method with the DF method using (a) the BK and (b) the Molière potentials.

The definition of  $k_{cl}$ , given by Eqs. (38) and (39), allows to use a classical cutoff not only for stripped ions but also for different interaction potentials. Hence, for the DF method, we show curves with and without the  $k_{cl}$  correction given by Eq. (39), with the use of the potentials given by Eqs. (27) and (32). It is clear from these figures that the introduction of the cutoff  $k_{cl}$  in the DF produces a significant improvement with respect to the plain dielectric formulation.

In Fig. 9(c) we show only the SPWS but for the BK and Molière potentials. Obviously, the case  $\eta = 1$  corresponds to fully ionized particles screened by a Yukawa potential, and so

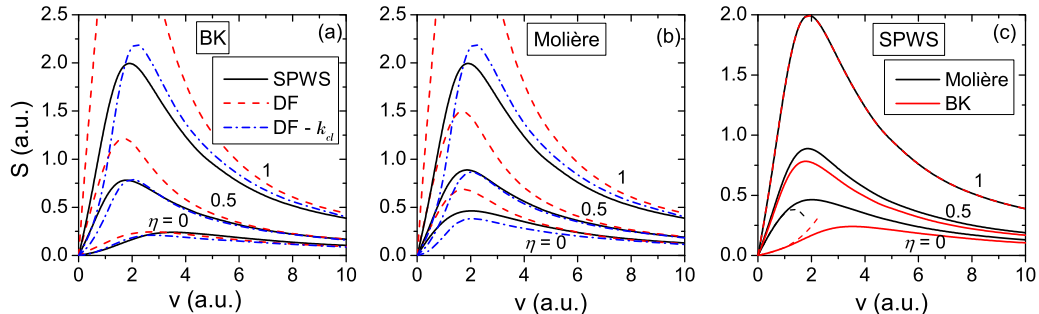


FIG. 9. Stopping of carbon for different ionization degrees  $\eta$ . We compare projectile models (BK and Molière) and stopping calculation (SPWS and DF) methods.



both ion models coincide. The dashed lines in this figure will be discussed in Appendix B.

## VII. CONCLUSIONS

Far from being a closed and well-described subject, the interaction of partially ionized projectiles with dense plasmas still presents several aspects that are not well described by the usual dielectric formulation in the form used in many publications. The incorporation of classical cutoff values in the momentum transfer integrals aiming to reconcile the dielectric formulation with the classical Bohr limit, when  $Ze^2/\hbar\bar{v}_r > 1$ , does not provide a consistent and well-behaved result in wide regions of plasma conditions, leading to a strong cancellation of the stopping power for a range of energies below the maximum.

We have explored in this work the limitations of the dielectric formulation when trying to describe some of those cases. As we have shown, the introduction of the Coulomb classical cutoff in order to amend the dielectric formulation may become physically unrealistic not only for highly charged ions but also for partially and neutral projectiles. The new classical cutoff criterion proposed here improves the behavior and shows that the failure of the dielectric calculation arises from the inappropriate cutoff criterion, which does not take into account the screening effects on the ion field.

So far the most reliable method that provides physically well-behaved solutions in all cases, with respect to both projectile and target conditions, is the full quantum mechanical calculation based on quantum scattering theory, or as was shown in previous work [9], the semiclassical scattering approach (SPWS). This approach provides an accurate solution to this problem and serves to obtain the correct behavior, even in the most complicated cases of partially dressed ions in high-density semidegenerate plasmas.

Using this approach and comparing the results with those of the dielectric calculations we have shown cases where (a) the quantum version of the dielectric method works quite well in its original form, (b) the quantum dielectric method requires the use of classical corrections to get appropriate results, and (c) even with the amendments of classical corrections, the dielectric method fails very badly [case of Fig. 5(b)]. In the last case we have identified the reason for the failure, which lies in the strong screening effects in the ion field of dressed projectiles or in high-density plasmas. Based on this analysis, we have proposed a modified cutoff criterion that considers screened interactions and improves the description in the low-energy range.

As a practical result of this analysis we have identified the regions on a density-temperature map where the previous versions of the dielectric formulations either work or fail.

We expect that the cases and limitations described in this work could serve as a warning for future calculations dealing with heavy ions in dense plasmas and could stimulate additional developments in this area.

## ACKNOWLEDGMENTS

This work was supported by the Comisión Nacional de Energía Atómica, CNEA (Controlled Nuclear Fusion Pro-

gram), Universidad Nacional de Cuyo, and ANPCYT, Argentina. C.F.C. acknowledges the support of the Consejo Nacional de Investigaciones Científicas y Técnicas (CONICET), Argentina.

## APPENDIX A: ON THE BETHE LIMIT IN THE QUANTUM FORMULATION OF THE DIELECTRIC FUNCTION

As we mentioned in the Introduction, the quantum formulation of the dielectric function, given in Sec. IV, already has a quantum cutoff limit in the  $k$ -integral. To illustrate this, we show in Fig. 10 the function

$$\mathcal{I}(\omega, k) = \omega \operatorname{Im} \left[ \frac{-1}{\epsilon(k, \omega)} \right],$$

which is the frequency integrand of Eq. (21), in a two-dimensional color map. As can be observed, the main contribution of this function is around the region given by the curve  $\omega = \hbar k^2/2m$ . First, we note that the frequency integral, in Eq. (21), goes up to  $\omega = kv$  (which is also shown in the figure). Then, when the second integral of Eq. (21) is performed, that is the  $k$ -integral, only the region up to  $k = k_{\text{qm}} = 2mv/\hbar$  contributes to the integral.

This behavior is a well-known property of the Bethe theory [42,43], but it is important to note that this property is fully incorporated in the quantum version of the dielectric function.

## APPENDIX B: SPWS STOPPING WITH A MAXWELLIAN-LIKE DISTRIBUTION FUNCTION

We show here that the electronic stopping power represented in Eqs. (12) and (13) can be reduced to a single integral when a Maxwellian-like distribution function is used (the same applies for the Fermi distribution). To show this, we recall that  $\vec{v}_r = \vec{v}_e - \vec{v}$  is the relative velocity of a plasma electron to the projectile. Then, defining

$$\vec{v} \cdot \hat{v}_r = v \cos \theta_r,$$

$$\vec{v} \cdot \hat{v}_e = v \cos \theta_e,$$

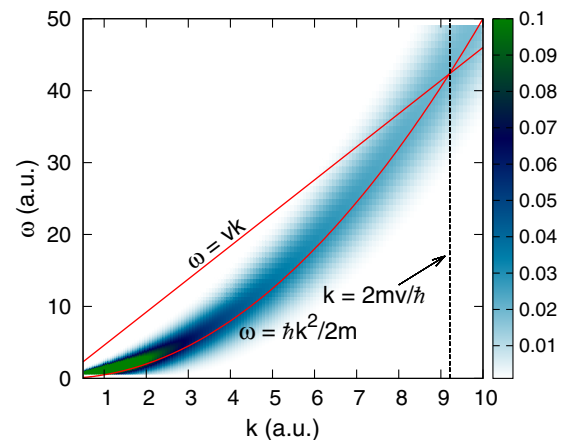


FIG. 10. Typical frequency integrand of the dielectric stopping power, given by Eq. (21) and using the quantum dielectric function. The figure shows how the Bethe limit is implicitly incorporated in this description.

we can rewrite Eqs. (12) and (13) to obtain [see also Eqs. (19) and following Ref. [8]]

$$S = 2\pi m n \int_0^\infty dv_e v_e^2 f(v_e) \int_0^\pi d\theta_e \sin \theta_e \cos \theta_r v_r^2 \sigma(v_r). \quad (\text{B1})$$

Then, using the relations

$$v_e^2 = v^2 + v_r^2 + 2vv_r \cos \theta_r, \quad (\text{B2})$$

$$v_e \cos \theta_e = v + v_r \cos \theta_r, \quad (\text{B3})$$

we change the integration variables from  $(v_e, \theta_e)$  to  $(v_r, \theta_r)$ :

$$S = 2\pi m n \int_0^\infty dv_r v_r^4 \sigma(v_r) \int_0^\pi d\theta_r \sin \theta_r \cos \theta_r f(v_e). \quad (\text{B4})$$

If the distribution function  $f(v_e)$  is a Maxwellian-like one, the angular integral can be analytically evaluated. In our case we use  $f_{MB^*}(v_e)$  and obtain

$$I(\beta) = \int_0^\pi d\theta_r \sin \theta_r \cos \theta_r f_{MB^*}(v_e) \quad (\text{B5})$$

$$= \frac{1}{\beta^2} [(1 + \beta)e^{-\beta} - (1 - \beta)e^{\beta}], \quad (\text{B6})$$

where  $\beta = vv_r/v_s^2$ . Finally, the stopping power takes the form of a single integral expression:

$$S = \frac{2\pi m n}{(2\pi v_s^2)^{3/2}} \int_0^\infty dv_r v_r^4 \sigma_{\text{tr}}(v_r) \exp\left(\frac{v^2 + v_r^2}{2v_s^2}\right) I\left(\frac{vv_r}{v_s^2}\right), \quad (\text{B7})$$

which presents a great numerical advantage taking into account that the full semiclassical phase shifts [Eq. (11)] require additional integrations for its calculation.

Using this expression, it is easily to expand the energy loss in powers of  $v/v_s$ :

$$S(v) = S_1 \frac{v}{v_s} + S_3 \left(\frac{v}{v_s}\right)^3 + O(5) \quad (\text{B8})$$

with

$$S_1 = \frac{4\pi m n}{3} \int_0^\infty dv_r v_r^4 \sigma_{\text{tr}}(v_r) \frac{1}{(2\pi v_s^2)^{3/2}} \exp\left(\frac{-v_r^2}{2v_s^2}\right) \frac{v_r}{v_s} \quad (\text{B9})$$

and

$$S_3 = \frac{4\pi m n}{3} \int_0^\infty dv_r v_r^4 \sigma_{\text{tr}}(v_r) \frac{1}{(2\pi v_s^2)^{3/2}} \times \exp\left(\frac{-v_r^2}{2v_s^2}\right) \left(\frac{1}{10} \frac{v_r^3}{v_s^3} - \frac{1}{2} \frac{v_r}{v_s}\right). \quad (\text{B10})$$

This yields the two main coefficients of the low-energy stopping power, the friction term  $S_1$ , and a cubic curvature coefficient  $S_3$ . Figure 9(c) shows this expansion, with dashed lines, for the neutral case ( $\eta = 0$ ).

For stripped and partially ionized projectiles, the cross section also depends on the projectile velocity  $v$  through the screening length  $\lambda(v)$ . Hence, for this case, Eq. (B8) is valid only for  $v \ll v_s$ . In particular, in this limit we can represent the transport cross section in terms of the collisional logarithm  $\ln \Lambda$ , in the usual way [8]:

$$\sigma_{\text{tr}}(v_r) = \frac{4\pi Z^2 e^4}{m^2 v_r^4} \ln \Lambda. \quad (\text{B11})$$

Then, if we assume an effective value for  $\ln \Lambda$  (independent of  $v_r$ ), the integral of  $S_1$  can be calculated immediately, and we retrieve a well-known expression first derived by Spitzer [6]:

$$S_1 \cong \frac{16}{3} \pi^{1/2} \frac{Z^2 e^4 n m^{1/2} v}{(2T)^{3/2}} \ln \Lambda. \quad (\text{B12})$$

Finally, we note that this approximation can be applied to a wide range of plasma parameters using the modified MB\* distribution.

- 
- [1] A. B. Zylstra, J. A. Frenje, P. E. Grabowski, C. K. Li, G. W. Collins, P. Fitzsimmons, S. Glenzer, F. Graziani, S. B. Hansen, S. X. Hu, M. G. Johnson, P. Keiter, H. Reynolds, J. R. Rygg, F. H. Séguin, and R. D. Petrasso, *Phys. Rev. Lett.* **114**, 215002 (2015).
- [2] J. A. Frenje, P. E. Grabowski, C. K. Li, F. H. Séguin, A. B. Zylstra, M. Gatu Johnson, R. D. Petrasso, V. Y. Glebov, and T. C. Sangster, *Phys. Rev. Lett.* **115**, 205001 (2015).
- [3] E. Fermi, *Phys. Rev.* **57**, 485 (1940).
- [4] D. Pines and D. Bohm, *Phys. Rev.* **85**, 338 (1952).
- [5] M. Gryziński, *Phys. Rev.* **107**, 1471 (1957).
- [6] L. Spitzer, *Physics of Fully Ionized Gases* (Interscience, New York, 1956).
- [7] S. T. Butler and M. J. Buckingham, *Phys. Rev.* **126**, 1 (1962).
- [8] L. de Ferrariis and N. R. Arista, *Phys. Rev. A* **29**, 2145 (1984).
- [9] C. F. Clauser and N. R. Arista, *Phys. Rev. E* **88**, 053102 (2013).
- [10] J. Lindhard, *Mat. Fys. Medd. K. Dan. Vidensk. Selsk.* **28**(8), 1 (1954).
- [11] R. H. Ritchie, *Phys. Rev.* **114**, 644 (1959).
- [12] J. Lindhard and A. Winther, *Mat. Fys. Medd. K. Dan. Vidensk. Selsk.* **34**(4), 1 (1964).
- [13] S. Skupsky, *Phys. Rev. A* **16**, 727 (1977).
- [14] N. R. Arista and W. Brandt, *Phys. Rev. A* **23**, 1898 (1981).
- [15] N. R. Arista, *J. Phys. C Solid State Phys.* **18**, 5127 (1985).
- [16] T. Peter and J. Meyer-ter-Vehn, *Phys. Rev. A* **43**, 1998 (1991).
- [17] E. M. Bringa and N. R. Arista, *Phys. Rev. E* **54**, 4101 (1996).
- [18] M. D. Barriga-Carrasco, *Phys. Rev. E* **88**, 043107 (2013).
- [19] M. D. Barriga-Carrasco, D. Casas, and R. Morales, *Phys. Rev. E* **93**, 033204 (2016).

- [20] S. Ichimaru, *Basic Principles of Plasma Physics: A Statistical Approach* (W. A. Benjamin, London, 1973).
- [21] N. A. Krall and A. W. Trivelpiece, *Principles of Plasma Physics* (McGraw-Hill, New York, 1973).
- [22] N. Bohr, *Mat. Fys. Medd. K. Dan. Vidensk. Selsk* **18**(8), 1 (1948).
- [23] J. D. Jackson, *Classical Electrodynamics* (John Wiley & Sons, New York, 1963).
- [24] N. R. Arista and W. Brandt, *Phys. Rev. A* **29**, 1471 (1984).
- [25] F. Bloch, *Ann. Phys.* **408**, 285 (1933).
- [26] G. Zwicknagel, C. Toepffer, and P.-G. Reinhard, *Phys. Rep.* **309**, 117 (1999).
- [27] N. R. Arista and P. Sigmund, *Phys. Rev. A* **76**, 062902 (2007).
- [28] L. D. Landau and E. M. Lifshitz, *Quantum Mechanics: Non-Relativistic Theory* (Pergamon Press, Oxford, 1960).
- [29] G. Maynard, G. Zwicknagel, C. Deutsch, and K. Katsonis, *Phys. Rev. A* **63**, 052903 (2001).
- [30] W. Brandt and M. Kitagawa, *Phys. Rev. B* **25**, 5631 (1982).
- [31] A. Bohr, *Mat. Fys. Medd. Dan. Vid. Selsk.* **24**(19), 1 (1948).
- [32] G. Molière, *Z. Naturforsch. A* **2**, 133 (1947).
- [33] N. R. Arista, *Nucl. Instrum. Methods Phys. Res. B* **195**, 91 (2002).
- [34] C. Deutsch and G. Maynard, *Phys. Rev. A* **40**, 3209 (1989).
- [35] S. Mabong, G. Maynard, and K. Katsonis, *Laser Part. Beams* **14**, 575 (1996).
- [36] G. Maynard, K. Katsonis, C. Deutsch, G. Zwicknagel, M. Chabot, and D. Gardès, *Nucl. Instrum. Methods Phys. Res. A* **464**, 86 (2001).
- [37] G. Maynard, S. Mabong, and K. Katsonis, *Laser Part. Beams* **14**, 587 (1996).
- [38] T. Kihara and O. Aono, *J. Phys. Soc. Jpn.* **18**, 837 (1963).
- [39] H. A. Gould and H. E. DeWitt, *Phys. Rev.* **155**, 68 (1967).
- [40] L. S. Brown, D. L. Preston, and R. L. Singleton, *Phys. Rep.* **410**, 237 (2005).
- [41] D. O. Gericke and M. Schlanges, *Phys. Rev. E* **60**, 904 (1999).
- [42] H. Bethe, *Ann. Phys.* **397**, 325 (1930).
- [43] M. Inokuti, *Rev. Mod. Phys.* **43**, 297 (1971).